

THE EFFECT OF TURBULENT PRESSURE ON THE P-MODE FREQUENCIES IN STELLAR MODELS

P. Demarque¹, L.H. Li¹, F.J. Robinson¹, S. Sofia¹, Y.-C. Kim², K.L. Chan³, and D.B. Guenther⁴

¹Center for Solar & Space Research, Yale University, New Haven, CT 06520-8101, USA

²Center for Space Astrophysics, Yonsei University, Seodaemoon-gu, Shinchon-dong 134, Seoul 120-749, Korea

³Mathematics Department, Hong Kong University of Science & Technology, Hong Kong, China

⁴Department of Astronomy & Physics, Saint Mary's University, Halifax, Nova Scotia B3A 4R2, Canada

ABSTRACT

We have constructed models for the sun at three stages of its evolution: a zero-age main sequence model, the present sun, and a subgiant model. For each model, the turbulent pressure and turbulent kinetic energy were calculated from 3-d radiative hydrodynamical simulations (described in the poster by Robinson et al.), and inserted into the 1-d stellar models. We note that in these simulations, the turbulent pressure is not a free parameter, but can be computed from the resulting velocity field. We show the calculated p-mode frequencies for the model of the present sun, with and without turbulent pressure, and compare them to the observed solar frequencies. When the turbulent pressure is included in the models, the calculated frequencies are brought closer to the observed frequencies in the sun by up to two μ Hz, strictly from structural effects. The effect of including turbulent pressure on p-mode frequencies is also shown for the zero-age main sequence model. Our models also suggest that the importance of turbulent pressure increases as the star evolves into the subgiant region. We discuss the importance of also including realistic turbulence as well as radiation in the non-adiabatic calculation of oscillation frequencies.

Key words: helioseismology; turbulence; p-modes.

1. INTRODUCTION

The purpose of this paper is to calculate the effect of including the turbulent pressure P_{turb} , derived from the 3-d radiative hydrodynamic simulations of Robinson et al. (described in a companion poster paper), into the hydrostatic structure of the outer layers of the models, where P_{turb} is known to be significant; and to determine the frequency shift caused by the inclusion of P_{turb} on the p-mode oscillation frequencies. The turbulent pressure was calculated

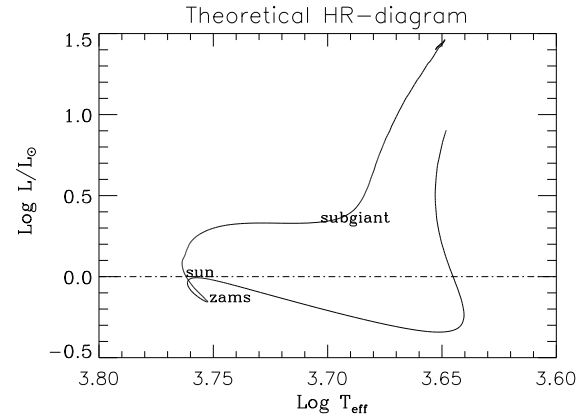


Figure 1. Evolutionary track for the sun from the pre-main sequence stage to the giant branch

for three models of the evolving sun, corresponding to the sun on the zero-age main sequence (ZAMS), the present sun, and the future sun as a subgiant.

2. EVOLUTIONARY MODELS FOR THE SUN

An evolutionary track for the sun was constructed which includes pre-main sequence evolution and post-main sequence hydrogen burning phases on the giant branch. The Yale Stellar Evolution code was used. We also adopted the standard assumptions for the calibration of the present sun as a standard solar model. The input physics included the OPAL opacities and equation of state, and the Alexander low temperatures opacities. Other physical assumptions were basically as described in Guenther & Demarque 1997). The evolutionary track is shown in the theoretical HR-diagram in Fig. 1.

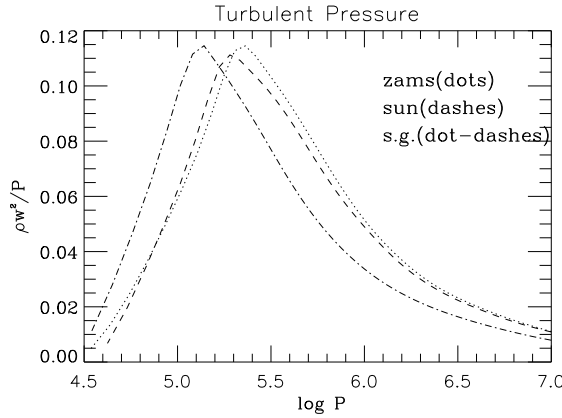


Figure 2. Fraction of turbulent to total pressure in the outer layers as a function of depth.

3. RADIATIVE HYDRODYNAMICAL 3-D SIMULATIONS

In order to better understand the structure of the atmosphere and of the highly superadiabatic layer (SAL) along the sequence, a number of 3-d radiative hydrodynamical simulations have been performed using the hydrostatic 1-d stellar models as starting points. The physics (thermodynamics and microscopic physics) in the simulation was performed in the same way as in the 1-d stellar models. These simulations follow closely the approach described by Kim & Chan (1998), and are described in more detail in the companion poster paper by Robinson et al. The full hydrodynamical equations were solved in a thin subsection of the stellar model, i.e. a 3-d box located in the vicinity of the photosphere. The radiative transport was treated in the following way:

- In the deep region of the simulation, where $dS/dz \approx 0$, the diffusion approximation was used.
- In the shallow region above, the 3-d Eddington approximation was used (Unno & Spiegel 1966).

After the simulation had reached a statistically steady state (see the poster paper by Robinson et al.), statistical integration was performed for each simulation, corresponding to over 2500 seconds in the case of the solar surface convection.

Some characteristics of the models are illustrated in Fig. 2 and Fig. 3. Fig. 2 shows a plot of the ratio of turbulent pressure ρw^2 to the gas pressure P as a function of $\log P$ (i.e. depth), in the convection simulations for the ZAMS model, the present sun and the subgiant model, respectively. We note that the peak in the turbulent pressure moves outwards, toward lower $\log P$, as the sun evolves.

Fig. 3 compares in addition the kinetic energy density for the two extreme cases of the ZAMS and sub-

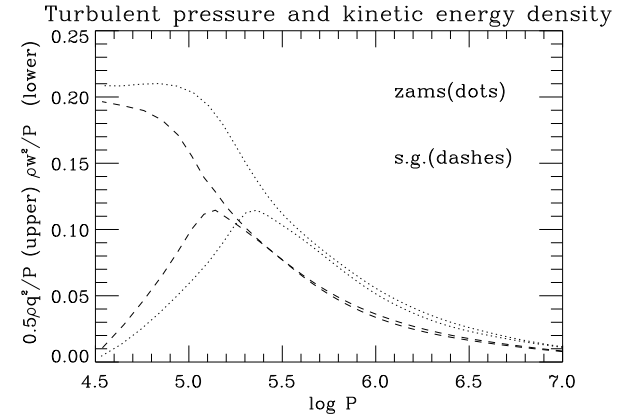


Figure 3. Comparison of the turbulent pressure and kinetic energy in the outer layers, for the two extreme cases, i.e. the ZAMS model and the subgiant model.

giant models, illustrating the effect of evolution on the atmospheric structure and dynamics.

4. INSERTING TURBULENT PRESSURE INTO 1-D STELLAR MODELS

From the 3-d hydrodynamical simulations, one can derive a turbulent pressure P_{turb} defined as $P_{turb} = \rho w^2$, where ρ is the mean density and w denotes the turbulent vertical velocity, i.e. the radial direction in the convection zone. The turbulent energy per unit mass is $\chi = 0.5q^2$, where $q^2 = u^2 + v^2 + w^2$, and the turbulent velocities u , v and w in the x , y and z directions respectively, are scaled by the sound speed at an arbitrary reference point.

Each parameter, which consists of a mean and a fluctuating part, is computed from the 3-d statistically averaged flow. For a given parameter X , the turbulent part is approximated by

$$x = \sqrt{\overline{X^2} - \overline{X}^2},$$

where the overbar denotes horizontal and temporal averaging, and X is the total quantity (mean plus fluctuating). The turbulent velocities u , v and w are all computed in this way.

In the 1-d stellar model, one can define a new parameter γ such that $P_{turb} = (\gamma - 1)\chi\rho$, by analogy with the treatment of magnetic pressure implemented by Li & Sofia (2000) in the Yale stellar evolution code. The total pressure is thus defined as, $P_T = P + P_{rad} + P_{turb}$, where P and P_{rad} are the gas and radiation pressures, respectively.

The equation of state is now written as $\rho = \rho(P_T, T, \chi, \gamma)$ while the energy conservation equation is modified by the inclusion of χ , so that

$$TdS_T = dU_T + P_T dV - (\gamma - 1)(\chi/V)dV.$$

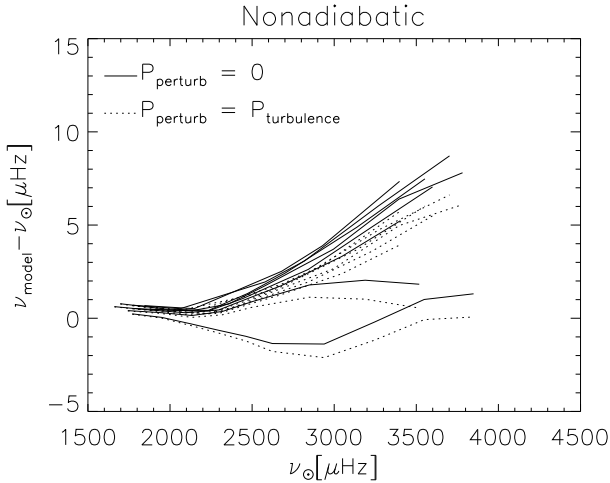


Figure 4. Difference between the present sun model and observed solar p-mode frequencies vs. observed frequency. Non-adiabatic frequencies are shown in this plot, for models with (dotted lines) P_{turb} and without (solid lines), for different l values.

5. EFFECT OF TURBULENCE ON P-MODE FREQUENCIES

The effects on the p-mode frequencies of introducing turbulent pressure in the stellar models is illustrated in Fig. 4, 5, 6 and 7. Fig. 4 and Fig. 5 refer to the model for the present sun, and Fig. 6 and Fig. 7 to the ZAMS model. The oscillation frequencies were calculated using the non-adiabatic oscillation code developed by Guenther (1994), which includes non-adiabatic corrections due to the effects of radiative processes. The difference between calculated p-mode frequencies and the observed solar frequencies for non-radial modes with $l = 30, 40, 50, 60, 70, 80, 90$ and 100 , are plotted vs. observed frequency. For each value of l , the frequency differences for standard solar models in which the P_{turb} is respectively ignored (solid lines) and included (dotted lines), are plotted.

We see in Fig. 4 and Fig. 5 that including P_{turb} reduces the model frequencies by approximately $2 \mu\text{Hz}$ at the higher frequencies. Since the effect of turbulence is only significant near the surface, the shift is the largest at the highest frequencies. The frequency shift is in the sense of improving agreement between calculated and observed solar frequencies (Antia & Basu 1997; Demarque et al. 1999).

We point out that Fig. 4 and Fig. 5 show the p-mode frequency shifts due to structural changes in the stellar models, but do not include frequency shifts which might be due to turbulence in the calculation of the oscillation frequencies. As mentioned above, while radiation is included in Guenther's non-adiabatic frequency calculations, no account is taken of the Reynolds stress due to turbulence.

Balmforth (1992) has investigated the effect of turbulence, and found it to be relatively larger than the

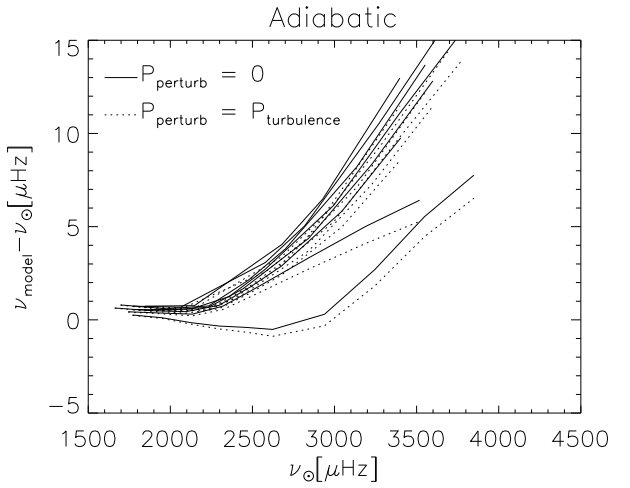


Figure 5. Same as Fig. 4, using adiabatic frequencies.

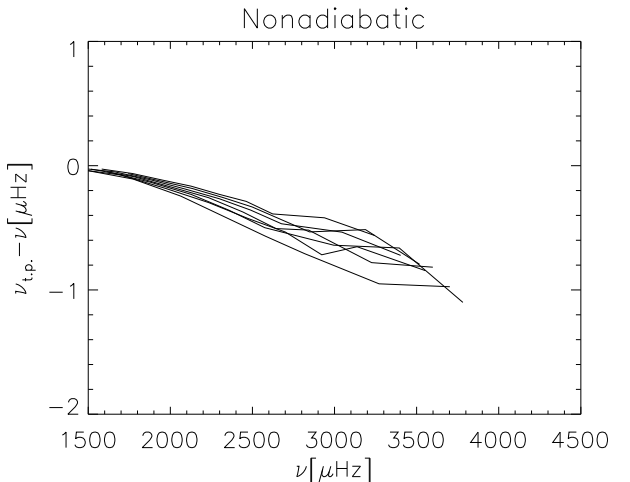


Figure 6. Frequency differences between ZAMS models with and without P_{turb} , plotted vs. frequency. Non-adiabatic frequencies have been used, for different l values.

structural effect on the calculated frequencies, of the order of $10 \mu\text{Hz}$. Guzik & Swenson (1997) found a shift of a few μHz only for low degree mode (l less than 10), and an increase of up to a few tens μHz for $l \geq 100$). More recent studies of the Reynolds stress correction on the p-mode frequencies have yielded smaller frequency shifts both using a simple mixing length model (Böhmer & Rüdiger 1999), and a model of convection which includes a more realistic turbulence energy spectrum (Bi & Xu 2000). An obvious next step is to consider the combined non-adiabatic effects of radiation and turbulence using the turbulent pressure derived from a 3-d physically realistic simulation.

Fig. 6 and Fig. 7 show the difference between the calculated p-mode frequencies for ZAMS models of the sun, with and without the effects of the turbulent pressure. We note that the effect of including the turbulent pressure in the ZAMS model is smaller than in the present sun model.

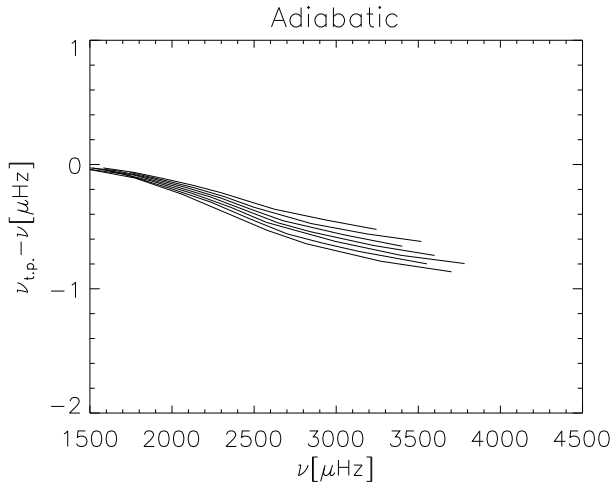


Figure 7. Same as Fig.6, but for adiabatic p -mode frequencies.

The simulation for the subgiant model indicate that the role of turbulent pressure increases as the star evolves toward the giant branch. This result is likely to be due to densities in the vicinity of the highly superadiabatic layer that are lower in giants than in main sequence stars.

Work is now in progress to extend this simulation grid, and to use the simulations to derive more realistic surface boundary conditions along evolutionary tracks than are currently provided by the mixing length theory of convection.

ACKNOWLEDGEMENTS

This research was supported in part by NASA grant NAG5-8406 to Yale University. Support from the Creative Research Initiative Program of The Korean Ministry of Science and Technology (Y.-C. Kim) and from the National Science and Engineering Research Council of Canada (D. B. Guenther) are also gratefully acknowledged.

REFERENCES

- Antia, H.M. & Basu, S. 1997 in SCORe'96: Solar Convection and Oscillations and their Relationship, p.51, eds. F.P. Pijpers, J. Christensen-Dalsgaard, C.S. Rosenthal (Kluwer:Dordrecht).
- Balmforth, N. 1992, MNRAS 255, 632.
- Bi, S. & Xu, H. 2000, A&A 357, 330.
- Böhmer, S. & Rüdiger, G. 1999 A&A, 351, 747.
- Demarque, P., Guenther, D.B. & Kim, Y.-C. 1999 ApJ, 517, 510.
- Guenther, D.B. 1994, ApJ 422, 400.
- Guenther, D.B. & Demarque, 1997, ApJ 484, 937.
- Guzik, J.A. & Swenson, F.J. 1997, ApJ 491, 967.

- Kim, Y.-C. & Chan, K.L. 1998, ApJ 496, L121.
- Li, L.H. & Sofia, S. 2000, ApJ in press.
- Robinson F.J. et al 2000, these proceedings.
- Unno, W. & Spiegel, E.A. 1966 PASJ 18, 85.